

Modeling of EUV Spectrum from Laser-Produced Sn Plasmas^{*)}

Akira SASAKI

Kansai Institute of Photon Science, National Institutes for Quantum Science and Technology, Kyoto 619-0215, Japan

(Received 24 July 2024 / Accepted 26 September 2024)

We investigate extreme-ultra-violet (EUV) emission from laser-produced tin plasmas for its application to microlithography. Strong emission occurs through 4d-4f and 4p-4d transitions, which appear as an unresolved transition array (UTA) due to the effect of configuration interaction (CI). Emissions from 8 to 13 times ionized tin overlap in the same $\lambda=13.5$ nm band, and both singly and multiply excited states of each ion contribute to the emission. We develop the collisional radiative model of tin ions, taking into account an appropriate set of atomic states that have a large population to contribute to the emission. The model is being validated through comparisons between the calculated and observed spectrums.

© 2025 The Japan Society of Plasma Science and Nuclear Fusion Research

Keywords: atomic processes in plasmas, plasma spectroscopy, EUV, lithography, multiply charged ion, tin

DOI: 10.1585/pfr.20.2401007

1. Introduction

The extreme ultraviolet (EUV) lithography is established based on the laser-pumped plasma source [1]. A small tin droplet is irradiated by a pair of pre-pulse and main pulse lasers to produce a plasma with an electron temperature of 20 to 50 eV. In the plasma, 8 to 13 times ionized tin shows broad emission from 4d-4f and 4p-4d UTA (Unresolved Transition Array) in the 13.5 nm band [2,3].

An EUV source with an output power of more than 500 W and convergence efficiency of 5 % has been obtained using the carbon dioxide laser as a pumping source [4]. However, improvements in power and efficiency are still required for future lithographic technologies, and the use of a more efficient solid-state laser is proposed [5]. We have been studying atomic processes of tin [6]. We extended the model to include the effect of multiply-excited states [7], with the method to identify states that significantly contribute to the emission [8]. In this work, based on the previous result of Y-like tin Sn^{11+} [9], we develop the model with 4 to 17 times ionized tin, and the emission spectrum is calculated and compared with the experiment by taking the effect of self-absorption into account.

2. Model

We investigate EUV spectrum from tin plasmas using the collisional radiative (CR) model [10] based on the configuration averaged (CA) levels. Figure 1 shows the energy level diagram of Sn^{11+} , which has a significant emission at $\lambda=13.5$ nm. The population of each atomic state n is calculated by solving a set of rate equations as,

$$\frac{dn_i}{dt} = \sum_j C_{i,j} N_e n_j + \sum_j A_{i,j} n_j - \left[\sum_k C_{k,i} N_e + \sum_k A_{k,i} \right] n_i, \quad (1)$$

where N_e is the electron density, $C_{i,j}$ and $A_{i,j}$ are collisional and radiative rate from j th state to i th state respectively. The population is calculated by taking atomic processes in plasmas into account, such as electron collisional ionization and excitation, three-body recombination and radiative recombination, autoionization and electron capture, and radiative decay. We use the energy levels, rate of radiative decay, and auto-ionization calculated using the HULLAC code [11]. On the other hand, we use empirical formulas to calculate the rate of collisional ionization, excitation, and radiative recombination. Rates of inverse processes such as three-body recombination and electron collisional deexcitation are calculated based on the detailed balance. Dielectronic recombination and excitation autoionization are taken into account by including multiply excited states above the threshold explicitly [9].

The population of tin ions is calculated by using the set of atomic states. A large number of multiply excited states are included to take their contribution to the EUV emission into account.

A group of excited states consisting of a common core with one excited electron is defined, and the number of groups is increased by choosing the core states according to their energy until the convergence is obtained [12].

The set of atomic states of each ion is determined recursively from the atomic states of the ion with one charge state above the target ion. For example, the atomic states of Y-like tin (Sn^{11+}) are produced from the atomic states of Sr-like tin (Sn^{12+}). The first group of atomic states of Y-like tin is produced by adding one electron to the ground

author's e-mail: sasaki.akira@qst.go.jp

^{*)} This article is based on the presentation at the 26th International Conference on Spectral Line Shapes (ICSLS2024).

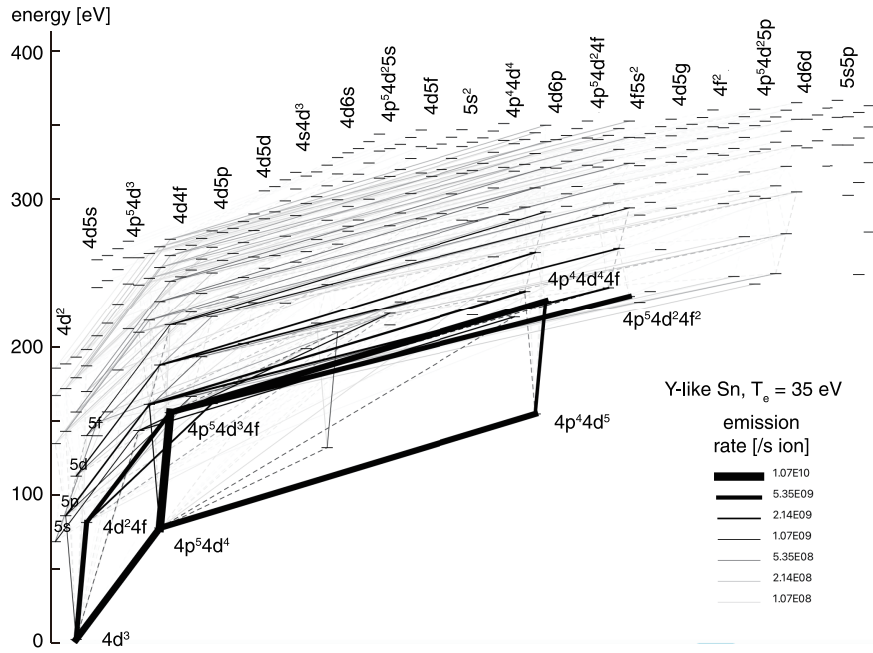


Fig. 1 Energy level diagram of Y-like Sn (Sn^{11+}). Lines between levels show the emission rate of UTA by their width and thickness, which is calculated at the electron temperature of 35 eV, assuming LTE.

state of Sr-like tin, $4d^2$ to produce $4d^2nl$, including the ground state of Y-like tin of $4d^3$. Then, the second group of atomic states of Y-like tin is produced from the first excited state of Sr-like tin, $4d5s$ to produce $4d5snl$. The sets of atomic states of Y-like tin are produced by taking the excited state of Sr-like tin according to its excitation energy. Subsequently, the energy of each state is calculated using the HULLAC and the excited states are chosen according to the order of excitation energy to have a set of core states to produce the atomic states of Zr-like tin (Sn^{10+}).

An atomic model typically includes 20 groups of excited states, as shown in Fig. 1, is used to calculate the population and emission spectrum, including transitions between multiply excited states such as $4p^44d^5 - 4p^4d^4$, $4p^54d^34f - 4p^4d^4$ and $4p^54d^24f^2 - 4p^54d^34f$, which have a greater contribution to the emission than transitions to the ground state such as $4d^24f - 4d^3$ and $4p^54d^4 - 4d^3$.

Finally, a collisional radiative model including Sn^{4+} to Sn^{17+} is developed, and the steady-state solution ($dn/dt = 0$) of the set of rate equations is obtained using the Monte Carlo method [12].

Calculation of the spectral emissivity and opacity is carried out using the population, taking the profile of UTA of Sn^{8+} to Sn^{13+} into account. Figure 2 shows the distribution of fine structure transitions for 4d-4f, 4p-4d, 4d-5p, and 4d-5f transitions to the ground state, which are calculated using the HULLAC. It is shown that due to the effect of CI, lines corresponding to 4d-4f and 4p-4d transition appear in the same 13.5 nm band and appear as a single UTA. The spectral emissivity and opacity are determined using the wavelength grid of 0.01 nm, which corresponds

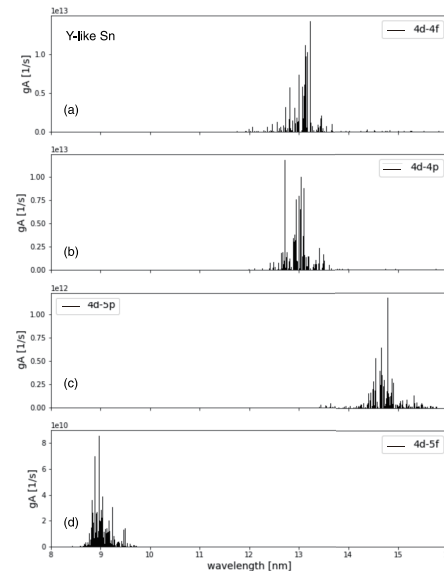


Fig. 2 Distribution of fine structure lines for (a) 4d-4f, (b) 4p-4d, (c) 4d-5p, and (d) 4d-5f UTA of Y-like tin (Sn^{11+}).

to the width of natural and collisional broadening of each fine structure transition.

The spectral profile of the EUV emission from laser-produced tin plasma is calculated in the presence of the effect of the opacity [13]. We use the escape probability of each UTA to calculate the spectrum [14]. For a uniform plasma sphere with the radius of r and spectral opacity of $\alpha(\lambda)$, the intensity of emission at the surface reduces as,

$$I(\lambda) = I_0(\lambda) \exp(-\alpha(\lambda)r). \quad (2)$$

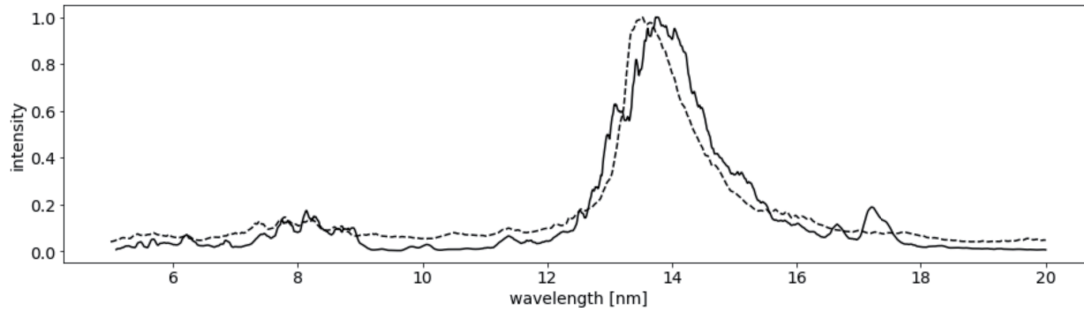


Fig. 3 Comparison of experimental (solid line) [5] and calculated (dashed line) spectrum. The experimental spectrum is obtained by irradiating the solid tin target with a YAG laser pulse with the intensity of 1.4×10^{11} W/cm² and the pulse duration of 15 ns. Calculations are carried out by changing the temperature, density, and radius the plasma.

Subsequently, the radiative rate A of UTA is reduced from the original value of A_0 by the probability of escape f_{esc} as,

$$A = \frac{A_0}{\Delta\lambda} \int_{\lambda_0 - \frac{\Delta\lambda}{2}}^{\lambda_0 + \frac{\Delta\lambda}{2}} \exp(-\alpha(\lambda)r) dr = f_{esc} A_0, \quad (3)$$

using the central wavelength λ_0 and width $\Delta\lambda$ of each UTA. The self-consistent emission intensity and population are obtained by iterative calculations. The effect of opacity causes the broadening of the EUV spectrum.

3. Result and Discussion

Figure 3 shows the calculated and observed EUV spectrum from a laser-pumped tin plasma. Calculations are carried out by changing the density and temperature of the plasma to compare it with the observation, and the best agreement is obtained at the ion density of 3.5×10^{18} 1/cm³ and electron temperature of 33 eV, assuming the radius of the plasma of 50 μ m,

It is found that the calculated spectrum reproduces the overall profile of the experimental as well as calculated spectrum by Torretti et al. [7] This result suggests that doubly excited states significantly contributing to the spectrum can be captured using the present algorithm-based method. Furthermore, in [7], the profile of UTAs was calculated taking full CI effects into account using a large set of configurations. In the present model, the profile was calculated with a relatively small set of configurations with the position corrected using experimental spectrum [6], suggesting that the simpler method might be useful for reproducing the experimental spectrum.

On the other hand, there are several differences in the detailed structure of the main peak at 13.5 nm, which arises from combined 4d-4f and 4p-4d UTA. For example, the calculated peak wavelength is 0.2 nm longer than the experiment. Agreement of the profile in the shorter wavelength of the main peak will be improved by taking the detailed spectral profile of 4p-4d transitions from Sn¹⁴⁺ and higher charged ions.

On the effect of opacity, in [7] the emission intensity

I_λ is calculated by a simple formula $I_\lambda = B_\lambda (1 - \exp(-\tau))$ where B_λ and τ_λ are spectral emissivity and optical depth, respectively, whereas we calculated the self-consistent population and radiation intensity. This difference will be investigated in the code comparison session in the EUV source workshop in the community of EUV source [15] and the theoretical model, computer codes, and data will further be validated.

Acknowledgments

This work is partially supported by JSPS grants 21H04460, and 23H01147. The author acknowledges useful discussions and supports from Dr. K. Tomita and Dr. Y. Pan in Hokkaido University, Dr. K. Nishihara in Institute for Laser Science in Osaka University, Dr. I. Murakami in National Institutes for Fusion Science. The author also acknowledges support from Dr. M. Ishino, Dr. K. Kondo, and Dr. T. Kawachi in National Institutes for Quantum Science and Technology.

- [1] "EUV Lithography", ed. V. Bakshi (SPIE press 2018).
- [2] M. Klapisch *et al.*, Phys. Rev. A **25**, 2391 (1982).
- [3] W. Svendsen and G. O'Sullivan, Phys. Rev. A **50**, 3710 (1994).
- [4] K. Hummler *et al.*, Proceedings of SPIE, Extreme Ultraviolet (EUV) Lithography XII, 12530V (2024).
- [5] R. Schupp *et al.*, Phys. Rev. Appl. **12**, 014010 (2019).
- [6] A. Sasaki *et al.*, J. Appl. Phys. **107**, 113303 (2010).
- [7] F. Torretti *et al.*, Nature Comm. **11**, 2334 (2020).
- [8] A. Sasaki, High Energy Density Phys. **9**, 325 (2013).
- [9] A. Sasaki, Appl. Phys. Lett. **124**, 064104 (2024).
- [10] "Modern Methods in Collisional-Radiative Modeling of Plasmas", Springer Series on Atomic, Optical, and Plasma Physics Book Series, 90, ed. Y. Ralchenko (Springer, 2016).
- [11] A. Bar-Shalom *et al.*, J. Quant. Spectrosc. Radiat. Transfer **71**, 169 (2001).
- [12] A. Sasaki, High Energy Density Phys. **32**, 1 (2019).
- [13] R. Schupp *et al.*, Appl. Phys. Lett. **115**, 124101 (2019).
- [14] Y.T. Lee *et al.*, Phys. Fluids B **2**, 11 (1990).
- [15] <https://euvlitho.com/upcoming-event/2024-source-workshop/>